IOP Publishing | Royal Swedish Academy of Sciences Physica Scripta

Phys. Scr. **T171** (2020) 014027 (5pp) https://doi.org/10.1088/1402-4896/ab45c0

# Estimation of ELM effects on Be and W erosion at JET-ILW

**I Borodkina[1,2], D Borodin[3], S Brezinsek[3], V A Kurnaev[2], A Huber[3], G Sergienko[3] and JET Contributors[4,5]**

[1] National Research Nuclear University (Mephi), Kashirskoe sh.,31, Moscow, Russia
[2] Institute of Plasma Physics of the CAS, Prague, Czech Republic
[3] Forschungszentrum Jülich GmbH, Institut für Energie- und Klimaforschung—Plasmaphysik, Partner of the Trilateral Euregio Cluster (TEC), D-52425 Jülich, Germany
[4] EUROfusion Consortium, JET, Culham Science Centre, Abingdon, OX14 3DB, United Kingdom

E-mail: ieborodkina@mephi.ru

Received 1 July 2019, revised 30 August 2019
Accepted for publication 18 September 2019
Published 2 March 2020

**Abstract**

An important W erosion mechanism in JET divertor is the physical sputtering by both, impurity (e.g. Be) and hydrogenic ions hitting the W divertor with energies determined by the pedestal temperature during edge-localized modes (ELMs)—the so-called intra-ELM sputtering of W. The earlier developed analytical approach for the W divertor gross erosion estimation using the Langmuir probe measurements has been improved in this work taking into account the time-resolved pedestal temperature and density drop during the pedestal crash under intra-ELM conditions. The improved model allows reproducing the measured at the divertor tile particle and heat fluxes evolution at the effective magnetic connection length matched with the previous JET- ITER like wall (ILW) studies. The estimates for the tungsten sputtered flux in intra- and inter-ELM conditions for quasi-steady state plasmas executed at the end of the first year of JET-ILW operation (C30C experiment) show that Type I ELMs contribute significantly (~85%) to the gross tungsten erosion which is in a good agreement with the divertor optical emission spectroscopy (W I 400.9 nm line). ELM filament radial propagation is considered based on the advective-diffusive model and JET-C experiment results. The estimation for the ELM-induced local Be main chamber erosion at JET-ILW reveals the increase of the Be sputtered flux by 30% under intra-ELM conditions.

Keywords: JET, ITER-like wall, beryllium, erosion, pedestal, ELM

(Some figures may appear in colour only in the online journal)

## 1. Introduction

Estimation of plasma-facing materials sputtering during edge-localized modes (ELMs) is critical for the impurity production and operation of the next step device ITER. JET is equipped with the ITER-like wall (ILW) utilizing the same material combination: tungsten (W) divertor and beryllium (Be) main chamber. It provides the most relevant environment for ITER erosion studies including ELM-induced sputtering effects [1]. W impurity concentration in the core plasma of ITER just above $5 \times 10^{-5}$ can lead to unacceptable plasma cooling [2], therefore minimization and control of the W sputtering source is required. It was shown that W erosion in the JET divertor happens in general L-mode or inter-ELM phases mainly by Be impurity ions, as hydrogenic ion impact energies are on average below the W sputtering threshold [3]. However, the most important W erosion mechanism in JET divertor in H-mode plasmas is the intra-ELM sputtering by both impurity (e.g. Be) and hydrogenic ions with impact energies determined by the pedestal temperature [4].

In this paper the analytical approach for estimation of a W sputtered influx using Langmuir probe (LP) measurements under intra-ELM conditions is refined by taking into account the non-instantaneous change of plasma parameters in the pedestal

[5] See the author list of Emmanuel Henri Joffrin *et al* 2019 *Nucl. Fusion* **59** 112021 https://doi.org/10.1088/1741-4326/ab2276 'Overview of the JET preparation for deuterium–tritium operation with the ITER like-wall'.

 

during an ELM crash. The model was validated by the well-diagnosed series of JET-ILW type-I ELMy H-mode discharges providing a good data set for statistical analysis of the intra-ELM evolution of pedestal and target plasma profiles [5].

Experiments on Alcator C-Mod [6], DIII-D [7], ASDEX Upgrade [8], JET-C [9, 10] and other machines have shown that ELM filaments can reach the main chamber plasma-facing components (PFCs) and cause their local erosion increasing the impurity content in the scrape-off layer (SOL). It is essential to have a better insight into the main chamber plasma-wall interaction in present day tokamaks in order to provide reliable predictions of first wall erosion for next generation devices. Here, JET-C measurements of the main ELM-filament parameters from the graphite era (JET-C) (relevant measures in JET-ILW are not yet available) and the model for ELM filament radial propagation elaborated in [11] were applied to the JET-ILW allowing the quantification of the ELM filament induced local sputtering of the Be main wall JET limiters.

## 2. Improved model for an analytic approach for the W divertor intra-ELM erosion estimation

The 'LP-Analytic' analytic approach for the intra-ELM LP flux measurements interpretation in the divertor was suggested for restoring the initial velocity distribution of ions leaving the pedestal plasma during the ELM crash which depends on two free parameters: the initial ion temperature and the local magnetic connection length $L_{\rm con}$ [12]. In the frame of this approach using the Free-Streaming model assumptions for a non-collision parallel uniform ion transport to divertor during ELM [11, 13, 14] and assuming the shifted Maxwell ion parallel velocity distribution at the pedestal we simulate the ion flux profile at the target. Then matching it with LP measured profile the initial velocity distribution of ions leaving the pedestal during an ELM is restored. In the model developed earlier an instantaneous ELM source was assumed leading to the unrealistically high value of the local magnetic connection length [12]. In this paper a finite (non-zero) time of ELM burst and the dynamics of pedestal parameters during a pedestal crash are implemented leading to the correction (reduction) of the magnetic connection length. The improved model taking into account the time-resolved (TR) pedestal parameters is named as 'LP-Analytic-TR'. The expressions for the initial velocity distribution function of ions leaving the pedestal during an ELM and the particle and heat fluxes at the divertor target are derived for the specific values of pedestal temperature and density and then integrated over the time of ELM burst:

$$f(v_{\rm II}) = \left(\int_{-\Delta t_{\rm ELM}/2}^{\Delta t_{\rm ELM}/2} \frac{1}{\sqrt{\pi}\, c_s(\tau)} \cdot \exp \times \left(-\left(\frac{1}{c_s(\tau)} \cdot \frac{L_{\rm II}}{t-\tau} - 1\right)^2\right) {\rm d}\tau\right) / \Delta t_{\rm ELM}, \quad (1)$$

$$\frac{{\rm d}N}{{\rm d}t} = \left(\int_{-\Delta t_{\rm ELM}/2}^{\Delta t_{\rm ELM}/2} \frac{N_{\rm ELM}(\tau)}{\sqrt{\pi}\, c_s(\tau)} \cdot \exp \times \left(-\left(\frac{1}{c_s(\tau)} \cdot \frac{L_{\rm II}}{t-\tau} - 1\right)^2\right) \cdot \frac{L_{\rm II}}{(t-\tau)^2} {\rm d}\tau\right) / \Delta t_{\rm ELM}, \quad (2)$$

$$\frac{{\rm d}Q}{{\rm d}t} = \left(\int_{-\Delta t_{\rm ELM}/2}^{\Delta t_{\rm ELM}/2} \frac{M_i}{2} \frac{N_{\rm ELM}(\tau)}{\sqrt{\pi}\, c_s(\tau)} \cdot \exp \times \left(-\left(\frac{1}{c_s(\tau)} \cdot \frac{L_{\rm II}}{t-\tau} - 1\right)^2\right) \cdot \frac{L_{\rm II}^3}{(t-\tau)^4} {\rm d}\tau\right) / \Delta t_{\rm ELM}, \quad (3)$$

where $\Delta t_{\rm ELM}$ is the time of ELM burst duration assumed to be proportional to the characteristic time of the pedestal pressure drop during an ELM, $N_{\rm ELM}(\tau) = n_{e,\,\rm max}^{\rm ped} - \Delta n_e^{\rm ped}(\tau + \Delta t_{\rm ELM}/2)/(\Delta t_{\rm ELM})$ is the temporal dependence of the amount of particles leaving the pedestal, $T_e^{\rm ped}(\tau) = T_{e\rm max}^{\rm ped} - \Delta T_e^{\rm ped}(\tau + \Delta t_{\rm ELM}/2)/\Delta t_{\rm ELM}$ is the temporal dependence of the pedestal temperature and $c_s(\tau) = \sqrt{2kT_e^{\rm ped}(\tau)/M_i}$ is the ion sound speed at the pedestal. The TR evolution of pedestal parameters $N_{\rm ELM}(\tau)$ and $T_e^{\rm ped}(\tau)$ are obtained based on the coherently averaged type-I ELM pedestal temperature and density profiles [15, 16] during the 54 identical H-mode discharges from the two-week long JET-ILW operation ('C30C') with quasi steady-state wall conditions, where almost 900 s in H-mode was accumulated [5]. ELMs with $\Delta W_{\rm ELM} \sim 160$ kJ have appeared during the 6s-long flat-top phases of the discharges with frequency of about 30 Hz. This group of discharges allows to statistically analyze the intra-ELM evolution of pedestal and target plasma profiles which are used in this work.

Figure 1 presents the normalized to unity calculated particle (2) and heat fluxes (3) at the JET divertor bulk W horizontal outer tile (OT) for the 'C30C' parameters ($B = 2$ T, $T_{\rm ped} = 500$ eV, $n_{e,\rm ped} = 5 \times 10^{19}$ m$^{-3}$, $\Delta T_{\rm ped} = 300$ eV, $\Delta n_{\rm ped} = 1.5 \times 10^{19}$ m$^{-3}$, $\Delta t_{\rm ELM} = 0.8$ ms). One can see that the simulated profiles are in good agreement with the LP and infrared thermography (IR) measurements at the fitted magnetic field connection length of 500 m, which is consistent with the recent JOREK [17] simulations and ELM studies on JET and other tokamaks [18, 19]. It is found that accounting for pedestal dynamics and the non-instantaneous intra-ELM particle bursts leads to the broadening of the time of particle flux evolution at the target. The difference in the particle and heat flux waveforms is well reproduced by the model. Therefore, one can conclude that accounting for the pedestal temperature and density decrease at the pedestal crash during ELM in low density plasmas in fully ionising conditions allows obtaining the particle and heat fluxes at the divertor tile corresponding to the measurements at the magnetic connection length consistent with the JET-ILW studies ($L_{\rm II} = 500$ m) [17–19].

The W sputtering flux at the divertor OT during an ELM $\Gamma_{\rm W,ELM}$ and inter-ELM W sputtering flux $\Gamma_{\rm W,inter\text{-}ELM}$ for 'C30C' discharges can be analyzed as following:

$$\Gamma_{\rm WELM} \approx (\Gamma_{\rm ELM} - \Gamma_{\rm interELM}) \cdot (Y_{\rm D/W} + 0.005 \cdot Y_{\rm Be/W}) \Delta t \cdot f_{\rm ELM} \quad (4)$$

$$\Gamma_{\rm W,inter-ELM} \approx \Gamma_{\rm inter\,ELM} 0.005 \cdot Y_{\rm Be/W},$$

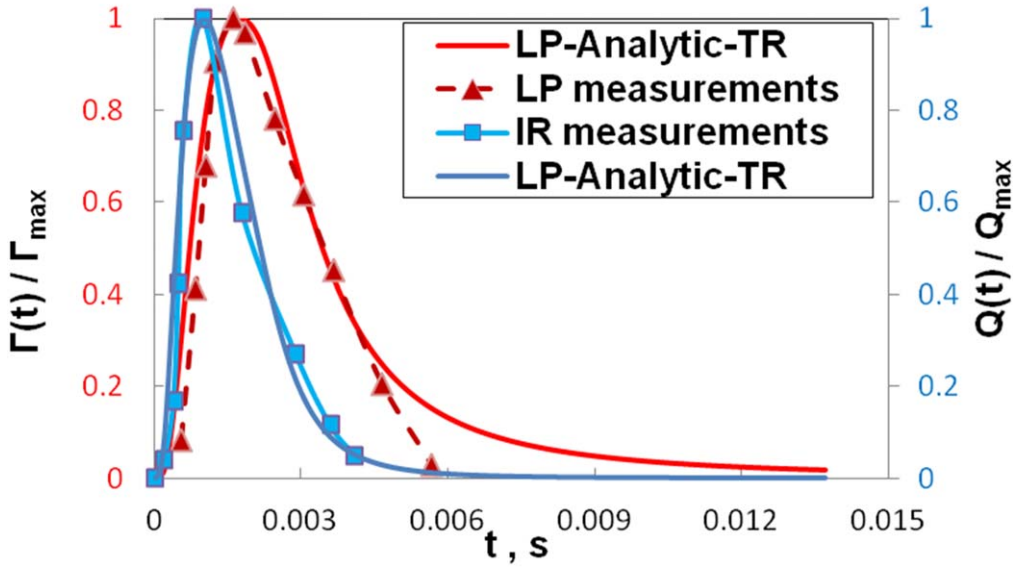


**Figure 1.** Simulated 'LP-Analytic-TR' and experimental particle and heat fluxes at the JET outer divertor target under the 'C30C' H-mode pulse type [5] intra-ELM conditions. The time evolution starting with the ELM pedestal crash beginning ($t = 0$) is reproduced including the difference in maxima position for the particle and heat fluxes.

where $\Gamma_{\mathrm{ELM}} = 3.4 \times 10^{23}\,\mathrm{s^{-1}\,m^{-2}}$, $\Gamma_{inter-\mathrm{ELM}} = 1 \times 10^{23}\,\mathrm{s^{-1}\,m^{-2}}$ are the measured by LP maximal ion fluxes at the bulk W outer horizontal target presented in [15], $f_{\mathrm{ELM}} = 30$ Hz—ELM frequency, $\Delta t = 2$ ms—time scale of LP flux profile at the half height, $Y_{\mathrm{D/W}}$, $Y_{\mathrm{Be/W}}$—the effective bulk W sputtering yields by $D^+$ and $Be^{2+}$ calculated by the Eckstein formula [20] using the respective ion impact energy and angular distributions simulated using the initial ion velocity distribution function (1) and the kinetic analytical expressions [21]. In inter-ELM conditions $Y_{\mathrm{D/W}}$ is neglected and only sputtering by $Be^{2+}$ ions is considered [3]. Following the previous Be migration studies for the unseeded type I ELMy H-mode experiments [3] the Be intrinsic plasma impurity concentration in the impinging ion flux is assumed to be around ~0.5% and consists mostly of $Be^{2+}$. The respective average $Y_{\mathrm{Be/W}}$ should be around ~0.07 for inter-ELM case with plasma parameters of $B = 2\,\mathrm{T}$, $n_e = 6 \times 10^{19}\,\mathrm{m^{-3}}$, $T_i = T_e = 35\,\mathrm{eV}$, $\alpha = 87^\circ$. However, during ELM $D^+$ ions have sufficient energy to significantly contribute to W sputtering [4, 21]. Under intra-ELM conditions the average W sputtering yield due to $Be^{2+}$ and $D^+$ should reach $Y_{\mathrm{Be/W}} \sim 0.57$ and $Y_{\mathrm{D/W}} \sim 1.4 \times 10^{-2}$, respectively, for plasma parameters $B = 2\,\mathrm{T}$, $n_e = 1.2 \times 10^{20}\,\mathrm{m^{-3}}$, $T_i = T_e = 35\,\mathrm{eV}$, $\alpha = 87^\circ$.

Finally, OT W sputtering sources retrieved from the LP measurements using the analytic approach have been compared to spectroscopic measurements of W I photon flux using photo multiplier tubes (PMT) with the 0.1 ms time resolution [22]. We took into account that the PMTs overestimate the tungsten signal by a factor of 2 due to contribution from the continuum background [4]. Unfortunately, due to the absence of one of the PMT-equipped LOS (at the OSP position) in 'C30C' no ELM-resolved W erosion at the exact spatial location of OSP is available. However, in the work [4] the analysis of different JET-ILW discharges showed that ELMs contribute 70%–80% to the overall W erosion, which allows estimating the intra-ELM W sputtering flux using the value of inter-ELM W flux. OT intra- and inter-ELM W sputtering fluxes estimated from both methods are given in table 1. Discrepancies between erosion fluxes do not exceed a factor ~2, which is rather good agreement taking into account the several assumptions and simplifications in the model as well as the issues of distinguishing the inter and intra-ELM light emission of sputtered species by spectroscopy method. The simulation shows that the Type I ELMs ($\Delta W_{\mathrm{ELM}} \sim 160\,\mathrm{kJ}$) contribute significantly (~85%) to the gross tungsten erosion, however the sputtered W ions can promptly re-deposit, therefore the intra-ELM W erosion models should also consider the re-deposition physics for net erosion estimates [23].

**Table 1.** Divertor outer target intra- and inter-ELM W sputtering flux for the 'C30C' discharges.

| Method | W I spectroscopy (400.9 nm line) | LP-Analytic-TR |
|---|---|---|
| ELM W flux (atoms $s^{-1}$) | (6.5–11.2) × $10^{19}$ | 2.4 × $10^{20}$ |
| Inter-ELM W flux (atoms $s^{-1}$) | 2.8 × $10^{19}$ [4, 22] | 3.8 × $10^{19}$ |
| ELM/ [Inter-ELM + ELM] | 70%–80% [4] | 86% |

## 3. Estimates for Be limiter sputtering flux during ELMs for 'C30C' experiment

Experiments on different tokamaks and numerical simulations show the filamentation of SOL plasma under intra-ELM conditions, leading to a creation of filamentary, field aligned structures, rotating toroidally/poloidally and moving radially. Infrared (IR) heat load measurements have showed that in specific cases up to half of the ELM energy was missing from

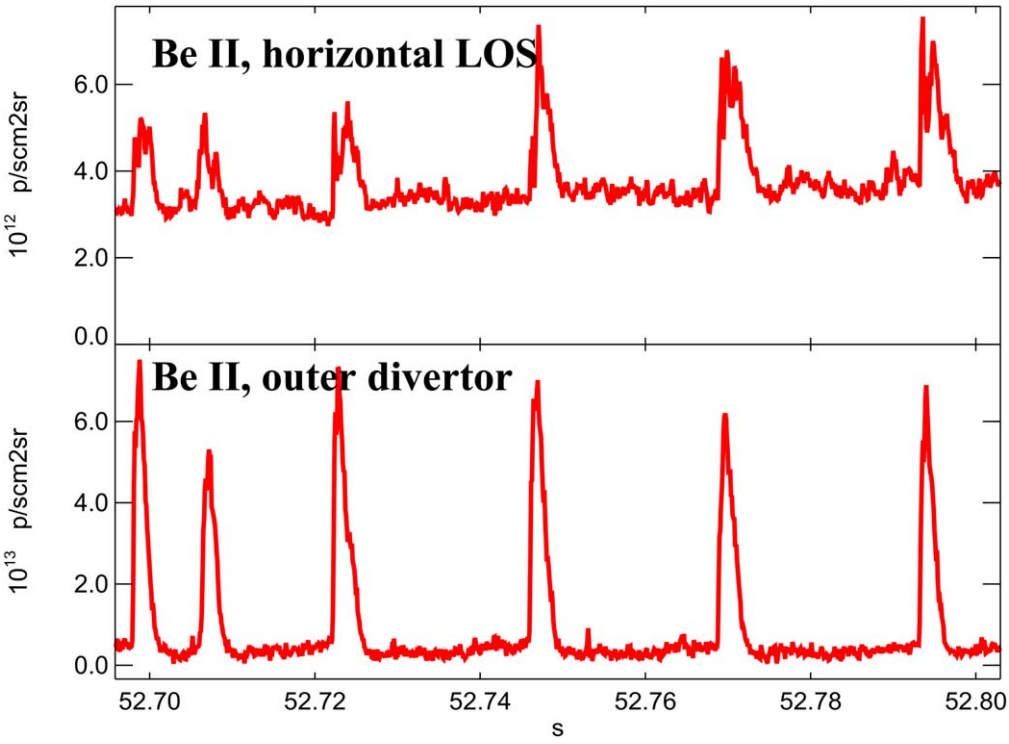


**Figure 2.** Clear correlation between frequencies of periodic Be II 527 nm line intensity peaks observed in the two LOS: the horizontal at midplane and the vertical directed to the outer divertor plate mimicking the ELM frequency in JET-ILW pulse 84782.

the divertor, and was presumably lost to the wall [24]. The ELM filament interaction with the first wall was also indicated in JET-C by the observed correlation between saturation current measured by the Retarding Probe above the outer midplane and the ELM frequency [10, 25]. In figure 2 a clear correlation between frequencies of periodic Be II 527 nm line intensity peaks is observed in the two lines of sight (LOS): the horizontal at midplane and the vertical directed to the outer divertor plate mimicking the ELM frequency in JET-ILW pulse 84782. Our interpretation is that the correlating peaks are due to erosion during the same ELM burst. According to the model of ELM filament propagation in SOL [11] the heat and particle fluxes during the pedestal crash are conveyed from the pedestal to the divertor targets by the parallel transport of the filaments along magnetic field lines and to the main chamber limiters by the radial propagation of the filaments due to the $E \times B$ radial drift. The average sonic timescale of the filament transport to the divertor is comparable with the ELM arrival time to the main chamber PFCs. Therefore the filament transport in both directions plays an essential role in ELM-evolution and should be included in the ELM-induced erosion studies.

An advective-diffusive model for ELM filament evolution in the SOL was elaborated in [11] by considering the conservation equations of mass and energy, together with parallel losses when the electrons cool more rapidly than the ions and the density is removed at the plasma sound speed. The Green's function of these equations, the response to a delta function impulse, yields a field-aligned, advective–diffusive, Gaussian wavepacket [11]. Its integral falls exponentially due to parallel losses, while the peak value is additionally decreased due to the filament broadening. Using this model and the experimental observations at JET-C we estimate the ELM incident ion flux to the outer limiters for JET-ILW 'C30C' conditions:

$$\Gamma_{\perp \mathrm{fil}} = n_e^{\mathrm{ped}} \cdot \exp(-\Delta_{\mathrm{SOL}}/\lambda_n) \cdot f_{\mathrm{broad}} \cdot v_r, \tag{5}$$

where the gap between the outer limiter and the LCFS ($\Delta_{\mathrm{SOL}}$) and the density $e$-folding length ($\lambda_n$) are equal to 6 cm and 13 cm, respectively, and the density peak reduction factor due to the filament broadening ($f_{\mathrm{broad}}$) is estimated as 0.33. The embedded LPs [10] and fast visible camera [26] showed that ELM filaments propagate radially with velocities ($v_r$) up to 2 km $\mathrm{s}^{-1}$, while the filament $T_e$ near the wall remains close to the inter-ELM level (25–50 eV) and $T_i$ drops from the pedestal by a factor of 3 [10, 25].

The Be sputtering flux under intra- and inter-ELM conditions is estimated using the incident ion fluxes and the respective Be sputtering yields:

$$\begin{aligned} \Gamma_{\mathrm{Be,ELM}} &\approx \Gamma_{\perp \mathrm{fil}} \cdot (Y_{\mathrm{D/Be}} + 0.005 \cdot Y_{\mathrm{Be/Be}}) \\ &\quad \times \Delta t_{\mathrm{ELM}} f_{\mathrm{ELM}} S_{\mathrm{wetted\_filament}} \\ \Gamma_{\mathrm{Be,inter\text{-}ELM}} &\approx \Gamma_{\perp \mathrm{inter\text{-}ELM}} \cdot (Y_{\mathrm{D/Be}} \\ &\quad + 0.005 \cdot Y_{\mathrm{Be/Be}}) \cdot S_{\mathrm{wetted\_lim}}, \end{aligned} \tag{6}$$

where the intra- and inter-ELM Be sputtering yields by $D^+$ and $Be^{2+}$ are calculated considering the pre-calculated incident energy and angle distributions and should reach 0.14 and 1.18, respectively, for intra-ELM filament conditions ($T_i$ = 170 eV, $T_e$ = 30 eV, $B$ = 2 T, $n$ = (1–1.5) × $10^{19}$ $\mathrm{m}^{-3}$) and 0.06 and 0.5 for inter-ELM conditions ($T_e = T_i$ = 10 eV, $B$ = 2 T, $n$ = 2 × $10^{18}$ $\mathrm{m}^{-3}$). The sputtering yields are calculated in the assumption of 50% D content at the Be limiters.

The inter-ELM ion flux to the main wall for 'C30C' conditions is $4.6 \times 10^{20}\,\mathrm{m^{-2}\,s^{-1}}$ according to the previous studies [5]. The inter-ELM wetted area $S_{\mathrm{wetted\_lim}}$ is estimated to be 10 times larger than the wetted area of the limiters by filaments $S_{\mathrm{wetted\_filament}}$ during an ELM calculated as follows:

$$S_{\mathrm{wetted\_fil}} = \frac{\Delta t_{\mathrm{ELM}}}{\Delta t_{\mathrm{fil}} + \Delta t_{\mathrm{sep}}} \cdot N_{\mathrm{lim}} \cdot \delta_{\mathrm{pol}}\,\delta_{\mathrm{lim}}, \qquad (7)$$

where $\delta_{\mathrm{pol}}$ is the filament poloidal size ~0.1–0.2 m, $\delta_{\mathrm{lim}}$ is the width of limiter ~0.2 m, $\Delta t_{\mathrm{ELM}} \sim$ 1–2 ms is the ELM duration, $N_{\mathrm{lim}} = 11$ is the number of the JET outer wall limiters, $\Delta t_{\mathrm{fil}} \sim 150\,\mu$s and $\Delta t_{\mathrm{sep}} \sim 300\,\mu$s are the temporal width and separation of filaments measured at JET [27]. The resulting Be source is found to be around $0.7 \times 10^{20}\,\mathrm{s^{-1}}$ for the intra-ELM conditions and $2.3 \times 10^{20}\,\mathrm{s^{-1}}$ for the inter-ELM conditions. One can conclude that Type-I ELM filaments lead to the local increase of the Be sputtered flux by 30% at JET-ILW conditions. This is in rather good agreement with the relative increase by 20% deduced from the spectroscopy measurements at the outer limiter in the figure 2 assuming the $S/$XB coefficients (conversion factors for the measured line intensity to the corresponding impurity flux from the wall) equal to 20 and 40 for inter- and intra-ELM conditions, respectively [4].

## 4. Conclusions

In this paper the analytical approach [12] for estimation of a W sputtered influx using Langmuir probe (LP) measurements is improved taking into account the TR (earlier was assumed instantaneous) temperature and density drop during the pedestal crash under intra-ELM conditions using the statistically analyzed pedestal parameter dynamics and divertor particle and flux measurements in the set of identical H-mode discharges during the two-week lasting JET ILW operation with quasi steady-state wall conditions [5]. The improved approach allows reproducing the measured particle and heat fluxes evolution at the divertor tile at the effective magnetic connection length matched with the previous JET-ILW studies.

Estimates of tungsten sputtered flux in intra-ELM and inter-ELM conditions show that Type I ELMs contribute significantly (~85%) to the gross tungsten sputtering which is in good agreement with the divertor optical emission spectroscopy at W I 400.9 nm atomic neutral tungsten line.

The effect of plasma filaments appearing during ELMs on the JET Be limiter erosion is assessed for the first time. The filament radial propagation is considered based on the advective-diffusive model and JET-C experiment results. The estimation for the ELM-induced local main chamber Be erosion reveals the increase of the Be sputtered flux by 30% under intra-ELM conditions. According to the experimental studies [7], a larger ELM amplitude or a smaller outer wall clearance should lead to an increase of the effective radial transport of particles and the fraction of the ELM particles reaching the main chamber PFCs. The enhanced Be content in the SOL plasma will probably increase the divertor erosion by the impurity transport inside filaments to the divertor. Moreover, for AUG, equipped with a W first wall, the ELM causes the main chamber erosion between (10–20)% of the divertor value [28] and the main wall impurity effect on intra-ELM divertor erosion can be much stronger than for JET-ILW with the Be main chamber. Therefore, the detailed modelling of the impurity ionization, trapping, thermalisation in filaments and subsequent transport to the divertor is required and will be considered in the future works.

## Acknowledgments

This work is supported by the Russian Science Foundation project № 18-72-00178. This work has been carried out within the framework of the EUROfusion Consortium and has received funding from the Euratom research and training programme 2014–2018 and 2019–2020 under grant agreement No 633053. The views and opinions expressed herein do not necessarily reflect those of the European Commission.

## ORCID iDs

S Brezinsek https://orcid.org/0000-0002-7213-3326

## References

[1] Matthews G F *et al* 2011 *Phys. Scr.* **T145** 014001
[2] Kallenbach A *et al* 2005 *Plasma Phys. Control. Fusion* **47** B207–22
[3] Brezinsek S *et al* 2015 *J. Nucl. Mater.* **463** 11–21
[4] Den Harder N *et al* 2016 *Nucl. Fusion* **56** 02601
[5] Brezinsek S *et al* 2013 *Nucl. Fusion* **53** 083023
[6] LaBombard B *et al* 2001 *Phys. Plasmas* **8** 2107
[7] Rudakov D L *et al* 2002 *Plasma Phys. Control. Fusion.* **44** 717
[8] Kallenbach A *et al* 2003 *Nucl. Fusion* **43** 573
[9] Goncalves B *et al* 2003 *Plasma Phys. Control. Fusion* **45** 1627
[10] Silva C *et al* 2009 *Plasma Phys. Control. Fusion* **51** 105001
[11] Fundamenski W *et al* 2006 *Plasma Phys. Control. Fusion* **48** 109–56
[12] Borodkina I *et al* 2017 *Nucl. Mater. Energy* **12** 341–5
[13] Moulton D *et al* 2013 *Plasma Phys. Control. Fusion* **55** 085003
[14] Guillemaut C *et al* 2016 *Phys. Scr.* **167** 014005
[15] Wiesen S *et al* 2017 *Nucl. Fusion* **57** 066024
[16] Harting D M *et al* 2015 *J. Nucl. Mater.* **463** 493–7
[17] Pamela S *et al* 2016 *Plasma Phys. Control. Fusion* **58** 014026
[18] Guillemaut C *et al* 2018 *Nucl. Fusion* **58** 066006
[19] Abrams T *et al* 2018 *Nucl. Mater. Energy* **17** 164–73
[20] Behrisch R and Eckstein W 2007 *Top. Appl. Phys.* **110** 33–187
[21] Borodkina I *et al* 2016 *Contrib. Plasma Phys.* **56** 640–5
[22] Brezinsek S *et al* 2016 *Phys. Scr.* **167** 014076
[23] Kirschner A *et al* 2019 *Nucl. Mater. Energy* **18** 239–44
[24] Eich T *et al* 2005 *J. Nucl. Mater.* **337–3 39** 669
[25] Pitts R 2006 *Nucl. Fusion* **46** 82–98
[26] Alonso J A *et al* 2007 *Proc. 34th EPS Conf. (Warsaw, Poland)* (ECA) P2-124
[27] Kirk A *et al* 2008 *J. Phys.: Conf. Ser.* **123** 012011
[28] Dux R *et al* 2011 *Nucl. Fusion* **51** 053002